# Transport properties in an InAs-inserted-channel In0.52Al0.48As/In0.53Ga0.47As heterostructure coupled superconducting junction



doi: 10.1103/PhysRevB.46.14286

RAPID COMMUNICATIONS

PHYSICAL REVIEW B VOLUME 46, NUMBER 21 1 DECEMBER 1992-I

# Transport properties in an InAs-inserted-channel $In_{0.52}Al_{0.48}As/In_{0.53}Ga_{0.47}As$ heterostructure coupled superconducting junction

Junsaku Nitta, Tatsushi Akazaki, and Hideaki Takayanagi
*NTT Basic Research Laboratories, 3-9-11 Midori-cho, Musashino-shi, Tokyo 180, Japan*

Kunihiro Arai
*NTT LSI Laboratories, 3-1 Morinosato Wakamiya, Atsugi-shi, Kanagawa 243-01, Japan*
(Received 24 July 1992; revised manuscript received 9 September 1992)

Supercurrent is observed in a superconductor-semiconductor-superconductor (S-Sm-S) junction using a two-dimensional-electron-gas system in an InAs-inserted-channel $In_{0.52}Al_{0.48}As/In_{0.53}Ga_{0.47}As$ heterostructure. The temperature dependence of the supercurrent cannot be explained by a simple exponential expression, but is here explained in terms of the clean-limit theory, taking account of the higher-order effect of the coherence length. The differential resistance of the junction shows clear subharmonic energy-gap structures due to multiple Andreev reflection since the phase coherence is maintained during the Andreev-reflection process. The Cooper pair transport explained by the clean-limit theory is attributed to the fact that the mean free path is longer than the coherence length and the length between the superconducting electrodes.

In recent years, much attention has been devoted to the superconductor-semiconductor-superconductor (S-Sm-S) system for device application[1] as well as for the study of mesoscopic Josephson effects such as a superconducting quantum point contact (SQPC).[2,3] In the SQPC, Andreev reflection at the S-Sm interface plays an important role. Furusaki and Tsukada have shown that the dc Josephson current is given by the Andreev-reflection amplitude and is carried by the discrete excitation bound states in the Sm region.[4] It is a challenging problem to combine the ballistic, phase-coherent transport in a two-dimensional electron gas (2DEG) with superconductivity. So far, the superconducting transport properties for S-Sm-S systems using an Si,[5] InAs inversion layer[6] and InGaAs (Ref. 7) have been explained in terms of the dirty-limit theory. Epitaxial InAs-coupled superconducting junctions are in the intermediate regime between the clean and dirty limits.[1] High supercurrent density was reported in an S-Sm-S junction using the AlSb/InAs quantum well system.[8] However, it has not been well verified that the supercurrent obeys the clean-limit theory. It is important to study the transport properties of the clean S-Sm-S systems to understand the ballistic transport coupled with superconductivity.

An InAs-inserted-channel $In_{0.52}Al_{0.48}As/In_{0.53}Ga_{0.47}As$ heterostructure[9] is attractive for an S-Sm-S system because 2DEG in the channel has both high electron density and high electron mobility, which provide the long coherence length and the long mean free path. Moreover, a good S-Sm contact is expected because there is no Schottky barrier between the superconducting electrodes and the InAs channel. This paper reports on the transport properties both in the superconducting state and in the finite voltage state of S-Sm-S junctions using the 2DEG in the InAs-inserted-channel $In_{0.52}Al_{0.48}As/In_{0.53}Ga_{0.47}As$ heterostructure.

The schematic structure of the fabricated junction is shown in Fig. 1(a), and the conduction-band structure is schematically presented in Fig. 1(b). A 2DEG channel is formed almost in the 4-nm InAs layer inserted into the undoped $In_{0.53}Ga_{0.47}As$ layer by optimizing the thickness and insertion position. The InAs-inserted-channel $In_{0.52}Al_{0.48}As/In_{0.53}Ga_{0.47}As$ heterostructure consists of a 200-nm undoped $In_{0.52}Al_{0.48}As$ buffer layer, a 13-nm Si-doped ($4\times10^{18}$ $cm^{-3}$) $In_{0.52}Al_{0.48}As$ layer, a 6-nm undoped $In_{0.52}Al_{0.48}As$ spacer layer, a 4-nm undoped $In_{0.53}Ga_{0.47}As$ layer, a 4-nm undoped InAs

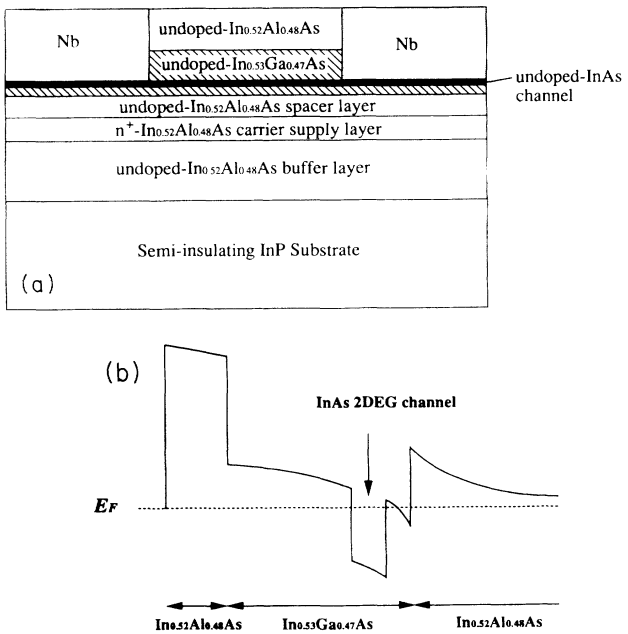


FIG. 1. (a) Cross-sectional view of the junction. (b) Schematic of conduction-band structure in an InAs-inserted-channel $In_{0.52}Al_{0.48}As/In_{0.53}Ga_{0.47}As$ heterostructure.

 

channel layer, a 12-nm undoped $In_{0.53}Ga_{0.47}As$ layer and a 20-nm undoped $In_{0.52}Al_{0.48}As$ layer. This $In_{0.52}Al_{0.48}As/In_{0.53}Ga_{0.47}As$ heterostructure was sequentially grown by molecular beam epitaxy (MBE) on a semi-insulating InP substrate. All $In_{0.53}Ga_{0.47}As$ and $In_{0.52}Al_{0.48}As$ layers are lattice-matched to InP. The carrier is supplied from $4\times10^{18}$ $cm^{-3}$ doped $In_{0.52}Al_{0.48}As$ layer to the channel layer. Two superconducting Nb electrodes, 100 nm thick, were defined by a lift-off process using electron beam lithography. Chemical etching was used to remove the 20-nm undoped $In_{0.52}Al_{0.48}As$ layer and the 12-nm undoped $In_{0.53}Ga_{0.47}As$ layer. The two electrodes were made by electron beam deposition after rf sputter cleaning in an evaporation chamber. The length $L$ between Nb electrodes was chosen in the range of 0.3–0.7 $\mu$m on the same chip. The electrode width $W$ is 80 $\mu$m

The $I$-$V$ characteristics of the junctions showed a clear supercurrent. The temperature dependence of the maximum supercurrent $I_c$ for an $L=0.3$ $\mu$m junction is shown in Fig. 2. The normal-state existence $R_n$ is 1.9 $\Omega$ at 4.2 K. To analyze this dependence, the carrier concentration $N_s$, mobility $\mu$, and effective mass $m^*$ of the $In_{0.52}Al_{0.48}As/In_{0.53}Ga_{0.47}As$ heterostructure were obtained. $N_s$ and $\mu$ were measured to be $3.0\times10^{12}$ $cm^{-2}$ and 41 000 $cm^2/V$ s, respectively, from Hall measurement at 77 K. A 2DEG with this carrier concentration is in the one-subband conduction state according to the band-structure calculation.[10] There is no experimental data for $m^*$ of an InAs-inserted-channel $In_{0.52}Al_{0.48}As/In_{0.53}Ga_{0.47}As$ heterostructure. The carrier concentration dependence of effective mass for $n$-type InAs (Ref. 11) has been experimentally obtained from the temperature dependence of the Shubnikov–de Haas oscillation amplitude. Therefore, we used $m^*=0.045$ at the same Fermi momentum $k_{F2}=k_{F3}$, where $k_{F2}$ and $k_{F3}$ are for the 2DEG and bulk InAs, respectively.

According to the theory of the superconducting proximity effect,[12] S-Sm-S systems are classified either as dirty systems, for $l<\xi_n$, or clean systems, for $l>\xi_n$ (where $l$ and $\xi_n$ are the mean free path and the normal coherence length of the semiconductor). The mean free path $l$ is given by $l=v_F\tau=\hbar\mu(2\pi N_s)^{1/2}/e$, where $v_F$ is the Fermi velocity and $\tau$ is the elastic scattering time. The coherence length $\xi_n$ is given by $\xi_{nc}=\hbar v_F/2\pi k_BT=\hbar^2(2\pi N_s)^{1/2}/2\pi m^*k_BT$ for the clean limit and $\xi_{nd}=(\hbar D/2\pi k_BT)^{1/2}=(\hbar^3\mu N_s/2k_BTem^*)^{1/2}$ for the dirty limit, where $D$ is the diffusion constant. It should be noted that the temperature dependence of $\xi_{nc}$ proportional to $1/T$ is different from $\xi_{nd}$, which is proportional to $(1/T)^{1/2}$. $\xi_{nc}$ depends only on $N_s$ and $m^*$, but $\xi_{nd}$ depends on $N_s$, $m^*$, and $\mu$.

From $N_s$, $\mu$, and $m^*$, the coherence length $\xi_n$ is $\xi_{nc}=0.32$ $\mu$m for the clean limit and $\xi_{nd}=0.43$ $\mu$m for the dirty limit at 4.2 K. The mean free path is 1.15 $\mu$m, which is more than twice as long as longer coherence length $\xi_{nc}$ and $\xi_{nd}$. It has been reported that the mobility at 15 K increases by 30% in $In_{0.52}Al_{0.48}As/In_{0.53}Ga_{0.47}As$ systems.[13] The actual $l$ and $\xi_{nd}$ at 4.2 K are expected to be longer than the above values. However, $\xi_{nc}$ is unchanged because the carrier concentration at 4.2 K is almost the same as at 77 K. Therefore, this S-Sm-S system is in the clean-limit region.

The dc Josephson current for low dimensional proximity systems was evaluated by Kresin.[14] According to the theory, $I_c$ is represented as

$$I_c \propto L^{-1/2}T\sum_{\omega_n>0}^{n}\frac{\Delta^2}{(\omega_n+\Delta^2)\omega_n^{1/2}}\exp\{-(2n+1)L/\xi_{nc}\}\ , \tag{1}$$

where $\Delta$ is the energy gap of the superconducting electrode at the interface and is evaluated by the self-consistent equation, and $\omega_n$ is given by $\omega_n=(2n+1)\pi k_BT$. This equation can hold in any temperature region and includes the higher-order effect of the coherence length. For the one-frequency approximation $n=0$, so Eq. (1) depends only on the usual coherence length $\xi_{nc}$ and a simple exponential expression.

This theory does not assume the barrier at the interface. As will be shown below, the contact between the 2DEG InAs channel and Nb is not perfect in the present sample. However, it is thought that the theory can be applied to our system because of the low barrier. Figure 2 compares the temperature dependence of $I_c$ with the theoretical results. The solid line in Fig. 2 corresponds to the calculated plot of Eq. (1) using 2DEG InAs parameters. The experimental results can be explained in terms of the Kresin theory with an assumption of $\Delta=1.0$ meV. It is thought that the quality of Nb is not so good at the beginning of Nb deposition. However, the reason for the reduction of the gap is not clear.

For comparison, the dashed line of the calculated plot using the one-frequency approximation is also represented in Fig. 2. In the lower-temperature region, the calculation cannot explain the experimental data. This discrepancy comes from the fact that $\xi_{nc}$ is longer than $L=0.3$ $\mu$m and the higher-order effect is not negligible at low temperatures. It is confirmed that the temperature dependence of $I_c$ for the junction with $l>\xi_{nc}>L$ can be explained by the clean-limit theory with the assumption,

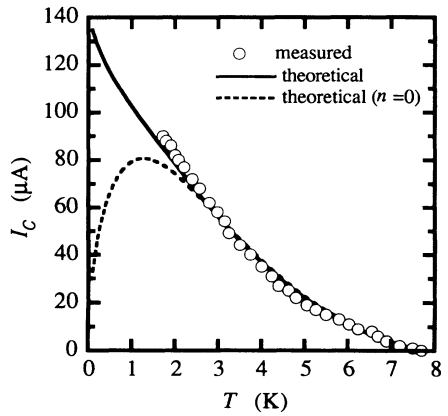


FIG. 2. Temperature dependence of $I_c$. The solid line is the calculated plot based on Eq. (1). The dashed line is the one-frequency approximation for $n=0$.

and the higher-order effect of the coherence length is not negligible.

Figure 3 shows the differential resistance as a function of voltage $dV/dI$-$V$ for an $L=0.63$ $\mu$m junction at 4.2 K. Dips were observed in the $dV/dI$ characteristics near voltages equal to $2\Delta/ne$, with $n=1,2,3$, where $\Delta$ is the bulk superconducting energy gap of Nb. These structures are subharmonic energy-gap structures (SGS's) due to multiple Andreev reflection. Very recently, clear subharmonic structures in $dV/dI$-$V$ characteristics were observed in the Nb-Si-Nb system,[15] which has the 0.05 $\mu$m length between the Nb electrodes. The length $L$ of our junction is much longer than that of the Nb-Si-Nb system. The sharp dip at zero voltage is due to the supercurrent of the junction.

The theoretical model to explain the subharmonic energy-gap structures was proposed by Octavio *et al.*[16] This model does not assume the elastic or inelastic scattering in the normal region and only elastic scattering at the interface is taken into account. The current through the junction is given by two nonequilibrium distribution functions which depend on their direction of motion, $f_{\rightarrow}(E)$ and $f_{\leftarrow}(E)$:

$$I=(eR_n)^{-1}\int dE[f_{\rightarrow}(E)-f_{\leftarrow}(E)]\ , \tag{2}$$

where $R_n$ is the normal-state resistance defined at a high voltage more than the superconducting energy gap. The shape of the differential resistance of the junction reflects the contact properties at the S-Sm interface. The contact properties are described by the dimensionless parameter $Z$, which represents the barrier strength and the elastic scattering at the interface. The nonequilibrium distribution function depends on the barrier strength $Z$. The barrier strength weakens the Andreev-scattering coefficient at the S-Sm interface, and reduces the supercurrent. Using the appropriate boundary conditions at the interface and symmetry arguments, the distribution function is given by the following expression:[17]

$$f_{\rightarrow}(E)=A(E)f_{\rightarrow}(E-eV)+B(E)[1-f_{\rightarrow}(-E-eV)]+T(E)f_0(E)\ . \tag{3}$$

This consists of an Andreev-reflection part, a normal reflection part, and a transmission part. $A(E)$, $B(E)$, and $T(E)$ are the coefficients of Andreev reflection, normal reflection, and transmission, respectively.[18] These coefficients depend on $Z$. The transmission part described using $f_0(E)$ represents the equilibrium Fermi distribution function because of the massive reservoir of the superconducting electrodes. The applied voltage $V$ is equally distributed over the two S-Sm interfaces. $I$-$V$ characteristics are obtained by solving Eq. (3) self-consistently and using Eq. (2).

The calculated $dV/dI$-$V$ characteristics are also shown in Fig. 3 by the dashed line. Here we assumed $Z=0.85$. The dips at the subharmonic energy-gap voltages in the experimental results are small compared with the calculated curve. The voltage across the sample which is the coplanar structure varies over the interface. This smears the structures.[19,20] However, the measured $dV/dI$-$V$ characteristics are well reproduced by this model.

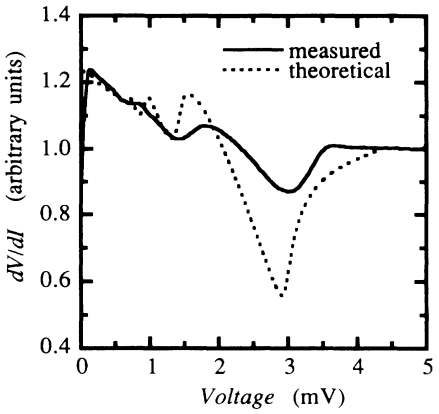


FIG. 3. Differential resistance as a function of voltage for the $L=0.63$ $\mu$m junction at 4.2 K. The dashed line represents the calculated plot with $Z=0.85$.

The typical $I_cR_n$ product of this junction, which represents the junction quality, is about 0.1 mV at 2 K. The $I_cR_n$ product is much lower than the superconducting Nb gap energy. There are two possible reasons for this low $I_cR_n$ product. One is due to the leakage current through the side area of the electrodes. The other is attributed to the low $I_c$ value because of poor contact.

The differential resistance of the junction tends to increase gradually below $2\Delta/e$, although it decreased in an Nb/InAs/Nb junction.[21] This means that the $Z$ value is larger than that of the Nb/InAs/Nb junction and the contact between the 2DEG InAs channel and Nb is not perfect. These results show that there is some barrier between the Nb electrodes and 2DEG InAs channel. Both $I_c$ and the $I_cR_n$ product are expected to be improved when there is good contact between Nb electrode and InAs channel. The Andreev-reflection coefficient for $Z=0.85$ is reduced to 0.17 at the Fermi energy. The low Andreev-reflection coefficient will disturb the formation of a discrete bound state due to Andreev reflection and also reduce the supercurrent.[4]

It is known that the inelastic scattering in the normal region smears the dips.[21,22] However, the observed subharmonic structures are clear and are explained by the theoretical model without assuming the inelastic scattering. This result comes from the fact that the mean free path of the channel is longer than the length $L$. The inelastic-scattering length is expected to be much longer than $L$, and the phase coherence is maintained throughout the conduction process. This shows that this S-Sm-S junction is in the mesoscopic region.

In conclusion, we have observed the supercurrent in the S-Sm-S junction using a 2DEG in the InAs-inserted-channel $In_{0.52}Al_{0.48}As/In_{0.53}Ga_{0.47}As$ heterostructure. The temperature dependence of $I_c$ can be explained by the clean-limit theory because the mean free path is longer than the coherence length. It also shows that the higher-order effect of the coherence length is not negligible for $\xi_n > L$. Differential resistance of the junction shows clear subharmonic energy-gap structures due to the multiple Andreev reflection since the phase coherence

is maintained during the conduction process. The superconducting transport properties explained by the clean-limit theory are attributed to the fact that the electron mean free path $l$ in the $In_{0.52}Al_{0.48}As/In_{0.53}GaZ_{0.47}As$ heterostructure is longer than $\xi_n$ and $L$. This is the first step toward the quantum transport effect of Cooper pairs such as an SQPC.

We thank Y. Ishii for his collaboration in this work and T. Enoki for his valuable discussion on a transport in the $In_{0.52}Al_{0.48}As/In_{0.53}Ga_{0.47}As$ heterostructure. We also thank T. Kawashima for the electron beam lithography and H. Nakano for assistance with the junction fabrication. We are also indebted to H. Hiratsuka, T. Izawa, and T. Kimura for their encouragement.

[1]T. Akazaki, T. Kawakami, and J. Nitta, J. Appl. Phys. **66**, 6121 (1989).

[2]A. Furusaki, H. Takayanagi, and M. Tsukada, Phys. Rev. Lett. **67**, 132 (1991); Phys. Rev. B **45**, 10 563 (1992).

[3]C. W. J. Beenakker and H. van Houten, Phys. Rev. Lett. **66**, 3056 (1991).

[4]A. Furusaki and M. Tsukada, Solid State Commun. **78**, 299 (1991).

[5]T. Nishino, E. Yamada, and U. Kawabe, Phys. Rev. B **33**, 2042 (1986).

[6]H. Takayanagi and T. Kawakami, Phys. Rev. Lett. **54**, 2449 (1985).

[7]A. W. Kleinsasser, T. N. Jackson, G. D. Pettit, H. Schmid, J. M. Woodall, and D. P. Kern, Appl. Phys. Lett. **49**, 1741 (1986).

[8]C. Nguyen, J. Werking, H. Kroemer, and E. L. Hu, Appl. Phys. Lett. **57**, 87 (1990).

[9]T. Akazaki, K. Arai, T. Enoki, and Y. Ishii, IEEE Electron Dev. Lett. **13**, 325 (1992).

[10]K. Arai, T. Akazaki, T. Enoki, and Y. Ishii (unpublished).

[11]T. Akazaki, J. Nitta, and H. Takayanagi (unpublished).

[12]P. G. de Gennes, *Superconductivity of Metals and Alloys* (Benjamin, New York, 1969).

[13]M. A. Tischler and B. D. Parker, Appl. Phys. Lett. **58**, 1614 (1991).

[14]V. Z. Kresin, Phys. Rev. B **34**, 7587 (1986).

[15]W. M. van Huffelen, T. M. Klapwijk, and L. de Lange, Phys. Rev. B **45**, 535 (1992).

[16]M. Octavio, M. Tinkham, G. E. Blonder, and T. M. Klapwijk, Phys. Rev. B **27**, 6739 (1983).

[17]K. Flensberg, J. Bindslev Hansen, and M. Octavio, Phys. Rev. B **38**, 8707 (1988).

[18]G. E. Blonder, M. Tinkham, and T. M. Klapwijk, Phys. Rev. B **25**, 4515 (1982).

[19]A. W. Kleinsasser, T. N. Jackson, D. McInturff, F. Rammo, G. D. Pettit, and J. M. Woodall, Appl. Phys. Lett. **57**, 1811 (1990).

[20]D. R. Heslinga, W. M. van Huffelen, and T. M. Klapwijk, IEEE Trans. Magn. **27**, 3264 (1991).

[21]J. Nitta, H. Nakano, T. Akazaki, and H. Takayanagi, in *Proceedings of the International Conference on Superconducting and Quantum Effect Devices and their Applications (SQUID'91)*, edited by H. Koch and H. Lubbig, Springer Series in Electronics and Photonics Vol. 31 (Springer, Berlin, 1991), p. 295.

[22]R. Kümmel, U. Gunsenheimer, and R. Nicolsky, Phys. Rev. B **42**, 3992 (1990).

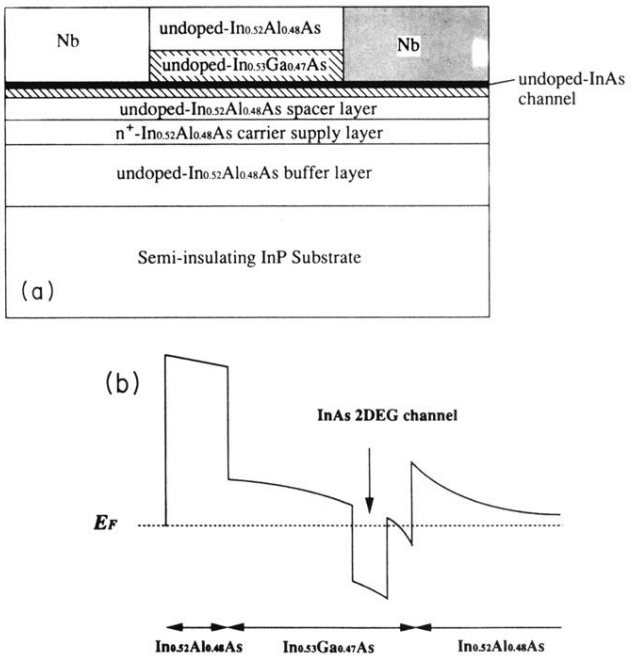


FIG. 1. (a) Cross-sectional view of the junction. (b) Schematic of conduction-band structure in an InAs-inserted-channel $In_{0.52}Al_{0.48}As/In_{0.53}Ga_{0.47}As$ heterostructure.